Spatiotemporal properties of auditory intensity processing in multisensor MEG

Article *in* NeuroImage · August 2014

DOI: 10.1016/j.neuroimage.2014.08.012 · Source: PubMed

NeuroImage 102 (2014) 465–473

Contents lists available at ScienceDirect

NeuroImage

journal homepage: www.elsevier.com/locate/ynimg

Full Length Articles

Spatiotemporal properties of auditory intensity processing in multisensor MEG

C. Wyss [a,b,*], F. Boers [a], W. Kawohl [b], J. Arrubla [a,c], K. Vahedipour [a], J. Dammers [a], I. Neuner [a,c,d], N.J. Shah [a,d,e]

[a] Institute of Neuroscience and Medicine, INM 4, Research Centre Jülich, Germany
[b] Department of Psychiatry, Psychotherapy and Psychosomatics, University Hospital of Psychiatry Zurich, Switzerland
[c] Department of Psychiatry, Psychotherapy and Psychosomatics, RWTH Aachen University, Germany
[d] JARA-Brain, Translational Medicine, Jülich, Germany
[e] Department of Neurology, RWTH Aachen University, Germany

ARTICLE INFO

Article history:
Accepted 5 August 2014
Available online 13 August 2014

Keywords:
Loudness dependence
Auditory evoked potentials
Magnetoencephalography
Posterior cingulate cortex
Serotonergic system
Cz

ABSTRACT

Loudness dependence of auditory evoked potentials (LDAEP) evaluates loudness processing in the human auditory system and is often altered in patients with psychiatric disorders. Previous research has suggested that this measure may be used as an indicator of the central serotonergic system through the highly serotonergic innervation of the auditory cortex.

However, differences among the commonly used analysis approaches (such as source analysis and single electrode estimation) may lead to different results. Putatively due to discrepancies of the underlying structures being measured. Therefore, it is important to learn more about how and where in the brain loudness variation is processed.

We conducted a detailed investigation of the LDAEP generators and their temporal dynamics by means of multichannel magnetoencephalography (MEG). Evoked responses to brief tones of five different intensities were recorded from 19 healthy participants. We used magnetic field tomography in order to appropriately localize superficial as well as deep source generators of which we conducted a time series analysis.

The results showed that apart from the auditory cortex other cortical sources exhibited activation during the N1/P2 time window. Analysis of time courses in the regions of interest revealed a sequential cortical activation from primary sensory areas, particularly the auditory and somatosensory cortex to posterior cingulate cortex (PCC) and to premotor cortex (PMC). The additional activation within the PCC and PMC has implications on the analysis approaches used in LDAEP research.

Introduction

The loudness dependence of the N1/P2 auditory evoked potentials (LDAEP) constitutes a prime object of investigation in the continuing search for biological correlates of psychiatric disorders (Kenemans and Kähkönen, 2011). Due to feasibility reasons the LDAEP is mostly recorded by electroencephalography (EEG). Nonetheless, the loudness dependence can also be measured from changes in magnetic fields (LDAEF) using magnetoencephalography (MEG). LDAEP has been reported to be a valid measure of central serotonergic neurotransmission both in animals and humans (Hegerl and Juckel, 1993; O'Neill et al., 2008). The basic concept of LDAEP is that serotonergic neurotransmission has a homeostatic function and modulates the responsiveness and sensitivity of cortical neurons in the primary auditory cortex (PAC) (Jacobs and Azmitia, 1992). A pronounced LDAEP supposedly reflects low central serotonergic neurotransmission, whereas a weak LDAEP reflects high serotonergic activity (Hegerl and Juckel, 1993; Kawohl et al., 2008; Wutzler et al., 2008). The measure of the auditory evoked response to increasing sound pressure levels is referred to as loudness dependence and is inter-individually different (Buchsbaum, 1971). The LDAEP has been widely applied in psychiatric samples (Ostermann et al., 2012; Park et al., 2010; Wyss et al., 2013), in studies with pharmaceutical challenge (Hitz et al., 2011; Kähkönen et al., 2002), in relation with the prediction of treatment outcome (Juckel et al., 2007; Linka et al., 2004) and in genetic association studies (Gallinat et al., 2003; Juckel et al., 2008; Kawohl et al., 2008).

Nonetheless, further improvement of the sensitivity and specificity of the LDAEP analysis is required to qualify it as a diagnostic marker. This could facilitate the clinical applicability of the parameter. Thus far the LDAEP has been analyzed in several different ways. The most common strategies used in EEG rely on single-electrode estimation (e.g. Debener et al., 2002), dipole source analysis (DSA; e.g. Wyss et al., 2013) and current source density analysis using low resolution brain

* Corresponding author at: Department of Psychiatry, Psychotherapy and Psychosomatics, University Hospital of Psychiatry Zurich, PO Box 1930, 8021 Zürich, Switzerland.
E-mail address: c.wyss@fz-juelich.de (C. Wyss).

http://dx.doi.org/10.1016/j.neuroimage.2014.08.012
1053-8119/

electromagnetic tomography (LORETA; e.g. Jaworska et al., 2013). A general restriction of source localisation in EEG and MEG is the existence of the inverse problem (Michel et al., 2004). This indicates that from the signal measured at the scalp, the location of the underlying generators is not uniquely determined. One should keep in mind that different source configurations can produce the same potentials on the scalp.

By using the EEG single-electrode estimation at the Cz electrode or the Fz electrode – by far the most used strategy to define the LDAEP – we have to account for following limitations: first, it is for sure that a single electrode cannot adequately represent source activity generated by the underlying brain area due to the superposition effect and the poor conductance of the skull. Secondly, using a single channel only is not possible to set apart the overlapping generators in both the primary and secondary auditory cortices with this approach. This differentiation is important because the serotonin concentration is highest in the primary sensory areas (Azmitia and Gannon, 1986; Juckel et al., 1997; Lewis et al., 1986). Positron emission tomography (PET) and autoradiography analysis showed a high mean density of serotonin transmitter receptors in the PAC (Fink et al., 2009; Zilles et al., 2002). Moreover, a functional magnetic resonance imaging (fMRI) study on LDAEP using individual landmarks for the separation of primary and secondary auditory cortices indicated different loudness dependencies in these areas (Brechmann et al., 2002). Thus, the primary auditory cortex plays a pivotal role in the analysis of the LDAEP and the consequential interpretations.

Fortunately, advances in source reconstruction allow for the isolation of the signal from the PAC in a relatively straightforward fashion. Both dipole source analysis (Hegerl and Juckel, 1993; Scherg and Picton, 1991) and LORETA (Mulert et al., 2002) showed to be capable of separating the sources in the auditory cortex and are used to determine the LDAEP. One problem with DSA is that the investigator has to define the number of dipoles that better explains the variances of contributing sources a priori. In the standard N1/P2 dipole model for the analysis of the LDAEP two dipoles are set in each hemisphere, one tangential dipole representing the PAC and one radial representing the secondary auditory cortex (Scherg and Von Cramon, 1985).

However, little effort has been made to specify if significant additional generators contribute to the scalp potential or account for an improvement of the residual variance in the dipole model. Electrophysiological studies conducted in the 1980s and 1990s already pointed out that the auditory N1 wave does not arise from a unitary source (i.e. auditory cortices) but reflects a superposition of sources with different functional significances (Giard et al., 1994; Knight et al., 1980; Näätänen and Picton, 1987; Picton et al., 1999). Those studies were mostly based on derived sources from the scalp potentials or limited by a priori dipole models. Since then not much research has been done on the underlying mechanism of auditory processing during the N1/P2 time window, even though the methodology has improved significantly. For instance, better resolution in space and time can be achieved by using a few hundreds of highly sensitive magnetometer sensors in MEG or by utilizing a hybrid fMRI/EEG system which provides both, high spatial and temporal resolutions (Neuner et al., under review).

Evidence from the recent studies comparing the diverging analysis methods in LDAEP research is in line with the assumptions that additional sources are activated. Hagenmuller et al. (2011) compared DSA analysis with single-electrode estimation within the same sample and found a significant difference between scores obtained with both methods. The authors assumed that a third source was additionally activated and contributed to the scalp signal captured by a single electrode. Actually, some studies used a third regional source in the dipole model in the frontal region, especially for high intensities in order to improve the residual variance between the modeled and the true signal recorded at the scalp (Hitz et al., 2011; Wyss et al., 2013). Surprisingly, a study by Mulert et al. (2002) compared DSA and LORETA for source localisation and did not find a significant correlation between the results of the two techniques. This dissociation could be explained because distinct types of source analysis methods were compared. DSA in contrast to LORETA is a discrete source analysis that requires a priori assumptions about the exact number of dipole sources based on physiological knowledge. In this study the authors used a two-dipole model instead of setting a third dipole. This could have led to a contamination of the true signal resulting from the tangential dipole activity representing the primary auditory cortex.

The present study aims at improving the analysis strategy of LDAEP investigations by taking into account all generators involved in loudness dependence by means of MEG analysis. We used wholehead MEG combined with a distributed source model approach which allows an exploratory analysis – without fixing the number of generators a priori – of the spatio-temporal profiles of the activated brain regions with excellent time resolution (Attal et al., 2012; Ioannides, 2006; Ioannides et al., 2004). The use of high-density recording by means of MEG/EEG has never been applied in the analysis of LDAEP thus far and the increased number of channels used in this study tend to result in a satisfactory disentanglement of the overlapping components in the brain (Dammers et al., 2007; Michel et al., 2004). We hypothesize that besides the auditory cortex additional sources contribute to late auditory evoked responses as observed from scalp recordings in the timeframe of N1m/P2m. We suppose that this interfering source activity is mostly apparent after high intensity tones due to the following reasons: First, while using dipole source models in the analysis of LDAEP an involvement of a third neuronal source was supposed to be present at particularly high intensities (Hitz et al., 2011; Wyss et al., 2013). Second, Näätänen and Picton (1987) already reported that an additional component was most easily observed at high intensities.

Our findings promise to be valuable in improving basic physiological knowledge of the involved processes in order to define prior assumptions in discrete source analysis, for instance to create an adequate dipole model (Scherg and Berg, 1991). Moreover, we intend to further elucidate the comparability of the various methodological approaches.

Materials and methods

Subjects

Nineteen healthy male right-handed subjects participated in the study (mean age 26.5 ± 4.0 years). All volunteers were recruited from the staff of the Forschungszentrum Jülich and from a volunteer mailing list. Subjects that met the following criteria were excluded: current or prior history of neuropsychiatric disorders as assessed by the Mini International Neuropsychiatry Interview (M.I.N.I.) (Sheehan et al., 1998); first-degree relatives with psychiatric disorders; drug or alcohol abuse; and smoking or a lifetime history of metabolic disorders. Subjects were instructed to consume neither alcohol nor any pharmaceuticals 48 h before or caffeine 12 h before measurements. Handedness was assessed by the Edinburgh Handedness Inventory (Oldfield, 1971). All subjects gave written informed consent. The study was approved by the Ethics Committee of the Medicine Faculty of the Rheinisch–Westfälischen Technischen Hochschule Aachen (RWTH Aachen University) and was carried out in accordance with the Declaration of Helsinki. One subject was excluded as not suitable for analysis because of poor signal quality from the MEG measurements which was most likely due to external noise.

Experimental procedure

Neuromagnetic field changes in response to auditory stimulation were recorded in a magnetically shielded room with a whole-head 248 magnetometer system (Magnes3600, 4D-Neuroimaging, San Diego, USA). Recordings were performed in a supine position with the

subjects lay with their eyes open. During the passive listening of the auditory stimulation all subjects were asked to stay relaxed and to avoid movements. As attention to the auditory stimuli has been shown to modulate the auditory evoked potentials (Schechter and Buchsbaum, 1973), and therefore also the LDAEP (Baribeau and Laurent, 1987), a silent movie was shown to the subjects for the purposes of distraction and they were told not to pay attention to the auditory stimuli. The sinusoidal tones (1000 Hz, 40 ms duration with 10 ms rise and fall time) were generated by a digital signal processor (Multi I/O Processor RX8, TDT System 3, Tucker–Davis Technologies, Alachua, USA) and were presented binaurally through earphones with plastic tubes and ear plugs inserted into the outer ear canals. Two programmable attenuators for the left and right ear (PA5, TDT System 3, Tucker–Davis Technologies, Alachua, USA) were used to present the tones at 10, 20, 30, 40, 50 and 60 dB sensation level (SL) in a pseudo-randomized order with not more than two equal levels following each other and pseudo-random stimulus onset asynchrony between 2 and 3 s in steps of 17 ms. Individual hearing thresholds were determined prior to each experiment and calibrated over five times. The mean threshold across all subjects was approximately 20 dB sound pressure level (SPL) and was just above the level of system noise of 20 dB SPL (at octave-band around 1000 Hz) that means that the presented stimuli were in the range of 30 to 80 dB SPL. The individual threshold was examined to guarantee an equal perception of the tones at both ears and to control the variability due to differences in the stimulation settings. Moreover, it is important to dissociate between perceived loudness and physical sound intensity, as it is supposed that the activation in auditory cortex rather reflects the subjective perception (Langers et al., 2007). A system specific constant time delay of 20 ms respective to the stimulus onset was taken into account and later subtracted for analysis.

MEG recording

The neuromagnetic activity was continuously recorded with a sampling rate of 678.17 Hz in a frequency range from DC up to 200 Hz. Prior to the MEG measurement, 5 head location coils were attached to subject's head. The position of the coils and the head itself was digitized using a 3D digitizer (Polhemus, 3space/Fastrack, Colchester, USA). Before and after each recording block, subject's head position was monitored by the head location coils, whereby a maximum difference of 5 mm for each experiment was accepted for further analysis. Eye movement and heart beats were monitored simultaneously using electrocardiography (ECG) and electrooculography (EOG), respectively (Brain Vision BrainAmp ExG MR, Brain Products, Gilching, Germany).

Individual anatomical MRIs

For the co-registration of the MEG coordinate frame with the individual brain anatomy, high-resolution T1-weighted MR-images were acquired for each subject with a voxel size of $1 \times 1 \times 1$ mm^3 (3T, Trio, Siemens, Erlangen, Germany). The rendered head shape was matched to the surface of the scalp by means of customized software, providing an affine transformation matrix for co-registering the MEG head coordinate and the MRI coordinate system (Dammers et al., 2007). For MEG source space preparation the individual anatomical brain was extracted using the Brain Extraction Tool (BET) as implemented in FSL (Version 5.0.4, FMRIB's Software Library, www.fmrib.ox.ac.uk/fsl) and a source space of approximately 10000–12000 nodes using an isometric 5 mm grid was defined prior to source analysis.

Data analysis

MEG signal processing

After acquisition, all data were band-pass filtered with a blackman windowed sinc filter (Smith, 1997) in the range of 1–200 Hz including notch filters at the power line frequency (50 Hz and the harmonics). Noisy MEG channels were excluded by visual inspection. Artifact rejection was automatically performed using the independent component analysis (ICA) as described in Dammers et al. (2008). Artifact free epochs were extracted for each stimulus in a time window ranging from −200 ms to +650 ms before and after stimulus onset, respectively. The epoch onsets were corrected for the time delay between generating and presenting the stimuli to the subject ears. A baseline correction was calculated from the pre-stimulus interval −200 ms to −50 ms. The first five epochs of each condition were excluded in order to reduce short-term habituation effects and epochs with threshold level above 3 pT were excluded by default. Within one subject, only the minimum number of accepted epochs (min. 70) was averaged according to the six conditions. Across subjects on average 73.8 (SD 1.3) out of 80 epochs were accepted for each condition and guaranteed an almost constant signal-to-noise ratio. Global field power (GFP) was calculated independently for each subject and condition and was normalized by dividing through the standard deviation of the baseline (Lehmann and Skrandies, 1980).

MEG source analysis

Magnetic field tomography (MFT; Ioannides et al., 1990) is a distributed source reconstruction method for the localization of the primary current density as recorded by MEG. MFT belongs to the family of weighted minimum norm solver (Ioannides, 2006; Ioannides et al., 1995; Taylor et al., 1999). A detailed description of the algorithmic steps is described in (Ioannides, 1995). In short: Let m_i be the output of the ith magnetometer. Then the measurement m_i can be expressed as a linear functional of the primary current density $j(r)$ with the vector-valued lead field $\phi_i(r)$ describing the sensitivity profile of the ith sensor:

$$m_i = \int_Q \phi_i(r) \cdot j(r) \cdot d^3 r. \quad (1)$$

For estimating the current density $j(r)$ MFT is based on a probabilistic treatment of the inverse problem where the estimated current density is expressed as a linear combination of expansion functions:

$$j(r) = \sum_k^N A_k \cdot \phi_k(r) \cdot w(r) \quad (2)$$

with N being the number of detectors, $w(r)$ is a probability weighting function defined throughout the source space, incorporating any a priori information about source location, and A_k are expansion coefficients that can be determined from the measurement data. In contrast to the well-known MN approach, MFT uses a non-linear weighting function $w(r)$ that allows the weights to depend on the strength of the first solution $||j_0(r)||^p$ (with $p = 1$) of the primary current density (Taylor et al., 1999). The initial values for the weighting function in MFT is determined by training the algorithm using computer generated data before MFT is applied to the real data (Ioannides et al., 1990). During inversion the weight update $w_n = c \cdot w_0(r) \cdot ||j_{n-1}(r)||^p$ is used to sharpen up the reconstruction within an iterative process, with w_0 being the initial weight and c being a constant to ensure that the sum of weights equals 1. In other words, the result of the first application is used to enhance the a priori probability weight in regions where the activity has been identified. The difference to MN estimation is that in MN-based solver no iteration is involved (with $p = 0$) and $w(r) = w = 1$. Moreover, the regularization parameter in MN solvers is estimated only once (typically from the noise covariance matrix), while in MFT the parameter is adapted for each inversion (Ioannides et al., 1990). In this way MFT is computationally more demanding, but is able to reconstruct shallow as well as deep sources at a time (Chen et al., 2009; Dammers and Ioannides, 2000; Weidner et al., 2010).

Lead fields used (cf. Eq. (1)) for the MFT analysis were computed from each individual subject with respect to a spherical head model.

Current density source reconstruction was estimated based on the averaged MEG data. We used the modulus (strength) of the current density activation for further analysis. The mean of the baseline was subtracted for baseline correction in each subject individually. Because we were only interested in calculating the root mean squared (RMS) values out of positive activations, negative values possibly resulting from baseline correction were set to zero. RMS values were calculated voxel-wise for these data for each subject in a sliding window of 50 ms latency with 25 ms overlap between 0 and 650 ms. In this way, full 3D reconstructions across time are provided with respect to the GFP distribution and the time characteristics of the auditory evoked components (Woods, 1995). These 4D spatio-temporal profiles (MFTrms values) were transformed into the Neuroimaging Informatics Technology Initiative (NIfTI) format using an interpolated common isometric voxel size of 2 mm^3 for both the MFTrms reconstruction and the MRI anatomical scans in order to combine the MFT solution with the FSL software. Each NIfTI-volume was then aligned to the MNI standard space (Montreal Neurological Institute, MNI152 2 mm brain) using the non-linear registration algorithm (FNIRT, Non-linear Image Registration Tool; FSL). Finally, the standard space volumes were used for statistical analysis throughout.

Statistical analysis

For group analysis, the transformed MFTrms volumes for each sound pressure level and time window were entered into second-level statistical group analysis using the generalized linear model included in FSL. Monte Carlo Permutation was applied as a non-parametric measure with minimal need of assumptions about the data. Due to our particular interest in the highest sound levels, we performed one-sample permutation t-tests with 5000 permutations to assess brain activity differences in the processing of the highest (60 dB) vs. lowest (10 dB) sensation levels (Nichols and Holmes, 2002). The voxel-wise maps were thresholded using threshold-free cluster enhancement (TFCE; Smith and Nichols, 2009) at $P < .001$ at cluster-level for $T = 3.73$ and all significance values were family-wise error (FWE) corrected for multiple comparisons. Variance smoothing was applied using a Gaussian kernel of width 3 mm in order to increase the power of the test. Anatomical regions were defined by means of the Jülich Histological Atlas (JHA; Eickhoff et al., 2006) at highest t-values and maximum probabilities of each anatomical label. For the regions that have not yet been defined in a cytoarchitectonic map, we used the macroscopic probabilistic Harvard–Oxford cortical structural atlas, provided with FSL.

We performed a time-course analysis within the anatomical regions significantly activated in the *t*-test during the N1m time window for each condition to elucidate the temporal dynamics across regions. Based on the 4D spatio-temporal profiles of the MFT analysis we calculated RMS values in space by taking into account all voxels in each of these regions-of-interest (ROI) for each time point. The data was normalized by the maximum value found across all conditions in time for each subject respectively, thus providing comparisons between subjects and conditions.

In order to statistically evaluate the best fit lines (linear or quadratic) of the slopes generated from mean RMS activations versus intensity levels (Fig. 3) across the ROIs, we used hierarchical linear regression analysis (SPSS version 22 for Mac) using RMS values as the dependent measure.

Results

Source analysis

Fig. 1 shows the GFP over 248 magnetometers of the averaged auditory evoked field calculated across all sound pressure levels. Based on these latency peaks we concentrated on the activity in the following time windows 75–125 ms for N1m and 175–225 ms for P2m.

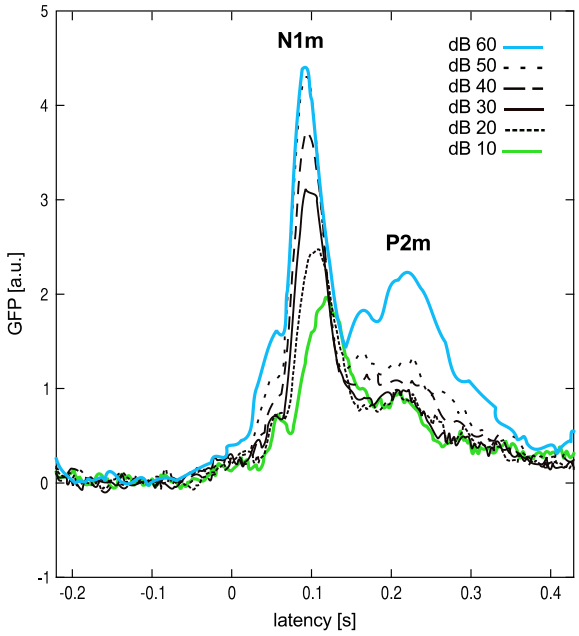

Fig. 1. Group averages (n = 19) of global field power (GFP) after auditory stimuli presentation (10–60 dB SL). The N1m peak occurred between 75 and 125 ms, the P2m peak between 175 and 225 ms. MFT analysis were conducted within these time windows. Reference level of intensity is SL.

In the N1m time window we found significant neural activations in the primary auditory cortex (PAC), the posterior cingulate cortex (PCC), the premotor cortex (PMC) and the primary somatosensory cortex (Fig. 2A). Moreover, activation was found in the paracingulate cortex. In the time window of P2m significant activations were shown in the PAC, the primary and secondary visual cortices extending into the precuneus and the PMC (Fig. 2C). Table 1 provides the t-contrast values and MNI coordinates.

Time course analysis of the activation in a ROI

The results of the time course analysis revealed different activation patterns among the ROIs between 0 and 300 ms (Fig. 2B). In the sensory cortices a saturation effect of the N1m could be observed that means that the highest sound level did not evoke a higher mean MFTrms value. According to latencies, the N1m component peaked between 88 and 133 ms across all intensity levels in the sensory cortices (auditory and somatosensory) and the PCC (Table 2). The time courses of the mean MFTrms values in the PMC did not show accentuated peaks. However, a loudness dependency is still obvious and a maximum value at 119 ms for the 60 dB condition was reached.

Relating to the P2m component a distinct peak with the highest sound level is shown in the PCC. In the remaining ROIs the peaks were rather broad and flat, nevertheless showing an increase around 220 ms in the sensory areas whereas no clear peak was observed in the PMC.

The temporal sequence of activations for the highest sound pressure levels determined from the N1-peak latencies was from PAC and primary somatosensory cortex to PCC and finally to PMC (Fig. 2B, Table 2). The left and the right PAC were activated simultaneously (Table 2).

LDAEP slope differences among the ROIs

A supplemental research question arose during our analysis based on the observation of the saturation effect. Therefore, the slope of the loudness dependence of the RMS activation across all intensities was generated at the previously defined time window of N1m (75–125 ms) within each ROI. Fig. 3 shows that the mean

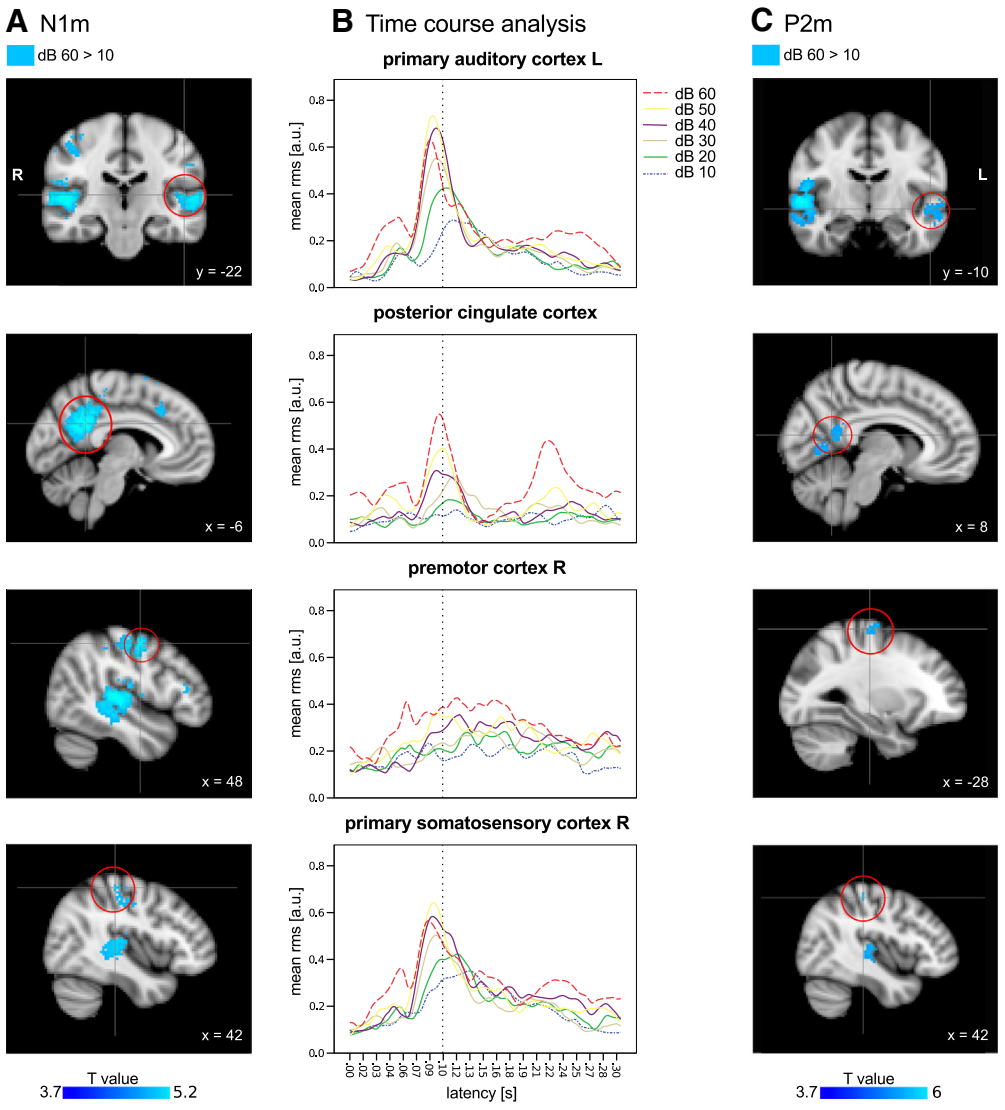

Fig. 2. MEG activation for the contrast analysis between the highest and the lowest intensity in the time window of N1m (A) and P2m (C) (N = 19, thresholded below P < .001 at cluster level for T = 3.73, FWE-corrected). Time course analysis between 0 and 300 ms poststimulus in each ROI (B). Vertical dotted line indicates the latency of N1. L: left hemisphere; R: right hemisphere. RMS values for time courses were low pass filtered at 30 Hz for graphical reasons. Reference level of intensity is SL.

MFTrms value in the PAC increases steadily with lower intensities but decreases with the highest intensity in both hemispheres. A similar trend was observed for the activation in the primary somatosensory cortex. On the other hand, the activation in the PCC and the PMC steadily increases with sound pressure level. These characteristics were confirmed by hierarchical linear regression analysis. Analysis revealed that a quadratic model was able to account for an additional amount of total variance of a linear model alone in the left and right

Table 1
Anatomical locations of all significant T-contrast activations in MEG magnetic field tomography in the time window of N1m and P2m (N = 19, thresholded below P < .001 at cluster level for T = 3.73, FWE-corrected). To keep apart the different clusters, local maxima within 10 mm of each other in each cluster were defined. L: left hemisphere; R: right hemisphere; k: cluster size; MNI: Montreal Neurological Institute (mm).

	Region	L/R	k	t-Value	MNI coordinates		
					x	y	z
	60–10 dB						
N1	Primary auditory cortex/planum temporale	R	2173	5.58	50	−26	6
	Primary auditory cortex/middle temporal gyrus	L	800	4.58	−50	−22	8
	Posterior cingulate cortex	L	2173	5.7	−6	−50	28
	Posterior cingulate cortex/precuneus	R	2173	5.4	4	−48	30
	Premotor cortex/primary somatosensory cortex	R	368	5.16	48	−6	50
	Paracingulate cortex	L	95	4.46	−4	20	44
P2	Primary auditory cortex	R	1651	6.42	52	−16	2
	Primary auditory cortex/middle temporal gyrus	L	385	4.34	−52	−10	−6
	Visual cortices V1 and V2/precuneus	R	212	3.85	8	−56	14
	Premotor cortex	L	117	4.59	−28	−20	66

Table 2
N1-peak latencies (ms) for each sound pressure level (dB SL) within ROIs. L: left hemisphere; R: right hemisphere.

Region		dB SL					
	L/R	10	20	30	40	50	60
		ms					
Primary auditory cortex/planum temporale	R	114	107	96	96	92	89
Primary auditory cortex/middle temporal gyrus	L	111	101	98	96	92	90
Posterior cingulate cortex/precuneus	L/R	117	111	117	96	104	99
Premotor cortex	R	88	172	200	121	96	119
Primary somatosensory cortex	R	133	120	95	92	93	88

PAC (left: $\Delta R^2 = .096$, $P = .000$; right: $\Delta R^2 = .083$, $P = 0.000$). No additional variances were explained for the quadratic model in the PCC ($\Delta R^2 = .003$, $P = .531$), PMC ($\Delta R^2 = .006$, $P = .378$) and in the primary somatosensory cortex ($\Delta R^2 = .018$, $P = .122$).

Discussion

This study assessed the neuroanatomical correlates of the N1m/P2m-complex evoked by the presentation of brief tones of different intensities. In addition to prior studies, multichannel MEG was used and source reconstruction was performed using a data-driven approach. Brain activation during the processing of the tones presented with the highest sound pressure levels compared to those with the lowest sound pressure levels was computed. However, the waveforms of both the N1m and P2m are not generated by a single region, but they rather reflect the sum of several relatively independent latent components generated by a distributed network involving PAC, primary somatosensory cortex, motor cortex and the PCC.

Sources in and near the auditory cortex

A large number of studies examined brain activity generated by loudness variation of auditory stimulation with EEG (Hegerl et al., 1994; Neukirch et al., 2002), MEG (Elberling et al., 1982; Vasama et al., 1995) or fMRI (Hart et al., 2002; Jäncke et al., 1998; Mulert et al., 2005). They have consistently found sources in and in the vicinity of the auditory cortex and further investigated the underlying neural mechanisms (i.e. increased responses or spatial extent of activated cortex volume) by intensity change. In line with these studies we found activation in the primary auditory cortex and specifically as shown in other MEG studies (Godey et al., 2001) the activation extended into the planum temporale at the N1m time-range (Table 1, Fig. 2). In contrast, the activation showed a slight posterior to anterior shift toward the planum polare in the time window of the P2m.

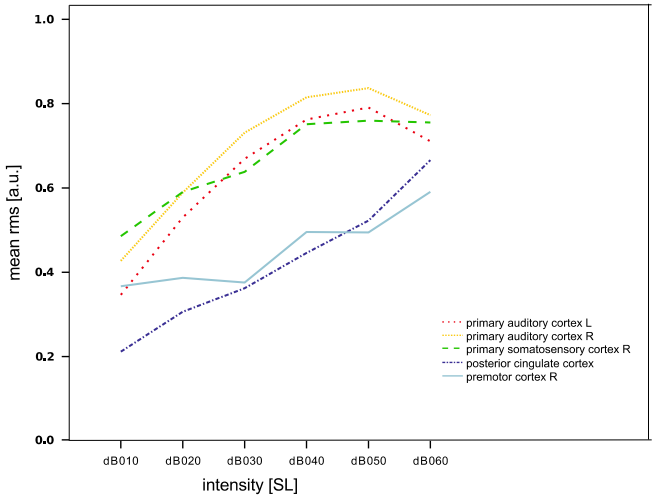

Fig. 3. ROI analysis of average current densities at N1m over all intensities. L: left hemisphere; R: right hemisphere.

Contribution of neural activity outside the auditory cortex

To our knowledge there is very little research reporting on sources outside the auditory cortex underlying the LDAEP. It is known that subcortical structures involved in the early processing of auditory stimuli such as the superior olive, the inferior colliculus and the medial geniculate body are sensitive to noise levels, showing a higher activity to increasing levels (Sigalovsky and Melcher, 2006).

Nevertheless, references from studies describing the generators of the auditory N1 and P2 components are extensive and should be taken into account for the interpretation of our results. Näätänen and Picton (1987) already pointed out that not only one predominant generator but also other sources contribute to the scalp recorded N1 peak in auditory processing. These authors proposed a third component underlying the N1 wave often referred as the "unspecific component" whose exact location is still unknown, but is proposed to lie within the frontal motor cortex and PMC in the precentral gyrus. Justification for these assumptions came from the effects of interstimulus intervals (ISI) on the scalp topography of the N1, as refractoriness processes become more active during increased ISI (>4 s) and thus lead to less specific additional sources near the vertex (Hari et al., 1982; Näätänen and Picton, 1987; Velasco and Velasco, 1986). Moreover, intracerebral recordings in monkeys supported additional generators of auditory evoked potentials in the PMC and motor cortex (Arezzo et al., 1975). Since then only few studies have contributed to the clarification of this third component by means of scalp current density and dipole analysis. The characteristics of this frontal response, however, are still ambiguous. Some authors (Alcaini et al., 1994; Giard et al., 1994; Näätänen and Picton, 1987) described a component with contributions from sources outside the auditory cortex with a peak latency of 100 ms, most easily recorded at intensities greater than 60 dB SPL and with long as well as short ISIs. The sources were described to lie within the posterior frontal lobe in the motor cortex (BA4), the supplementary motor area (BA6) or the cingulate gyrus. Other authors reported a component generated by the same regions but at later latencies (i.e. around. 125 ms; 140 ms) or with a longer refractory period, that is emerging only with longer ISIs (Alcaini et al., 1994; Picton et al., 1999).

Our study is the first using a distributed source model to show an additional significant activation in the PMC during the N1m time window. The response remained relatively constant between 60 and 180 ms and peaked at 119 ms in the condition of the highest intensity (Fig. 2). These findings are in agreement with the findings of the aforementioned previous work. The activation in the PMC might be related to the acoustic startle response to a sudden loud noise and is viewed as an aversive response to novel and potentially harmful stimuli (De Pascalis et al., 2012; Lang et al., 1990). The primary somatosensory cortex that is additionally activated in the present study could also play a considerable role in the processing of the startle response (Neuner et al., 2010). Other authors pointed out that the supplementary and premotor areas may be related to the orienting response, an orientation of attention to a change in the environment and linked to the planning and execution of motor

responses even though the subjects had no such task to perform (Hari et al., 1982; Kim et al., 1999; Näätänen and Picton, 1987).

Furthermore, the PCC was observed to belong likewise to the network of auditory intensity processing. The results show a greater increase in activation with higher sound pressure levels in the time window of N1m and P2m. Interestingly, one single LDAEP-study using PET reported activation in this region (Lockwood et al., 1999), but with maximal activation at lower intensities. The authors assigned to this region a significant role in regulating or controlling the magnitude of intensity and also mentioned a possible link to the attention system. However, the functional role of the PCC is currently not clear and competing theories exist (Leech and Sharp, 2014). According to our findings (Fig. 2B) the PCC is activated after the primary sensory areas and may subserve evaluative functions such as monitoring sensory events and homeostatic processes (Vogt et al., 1992). In fact, the PCC shows no direct innervations to primary sensory and motor areas (Parvizi et al., 2006), but connections to the prefrontal cortex. Interestingly, the PCC is modulated by serotonergic neurotransmission (Hahn et al., 2012). Long term treatment with selective serotonin reuptake inhibitors (SSRIs) were reported to have a significant effect on the neuronal structure (Kraus et al., 2014) and function (Matthews et al., 2010) of the PCC. Moreover, transmitter receptor fingerprints of the cerebral cortex indicate that the mean densities of 5-HT_{1A} and 5-HT_2 receptors are comparable between PCC and PAC (Zilles et al., 2002). While studies about treatment response prediction are promising in LDAEP research, the optimal used analysis method is still debated (Jaworska et al., 2013; Mulert et al., 2002; Park et al., 2011). However, scalp measured potentials, for instance at Cz, might reflect serotonergic modulated responses from both the PAC and the PCC (e.g. Linka et al., 2004). To our knowledge, there exists no study investigating a modulatory effect of the 5-HT system on the PMC.

Another interesting finding is that the presentation of auditory stimuli activated not only the primary auditory cortex but also the primary visual and somatosensory cortex. This is in agreement with the theory of multisensory integration that states low level integration in different sensory modalities (i.e. auditory, visual and somatosensory) and controverts the traditional assumption that multisensory integration is a higher order process (Schroeder and Foxe, 2005).

By comparing the activation pattern between the time windows of N1m and P2m, we did not find any significant differences (Table 2). Fig. 2 reveals that there has been a slight shift of activation from the PCC toward the precuneus and the visual cortices.

LDAEP slope differences among the ROIs

Our data showed that the characteristics of responses to high intensity levels differ between the ROIs. Responses at the highest intensities in the PAC level off, what is commonly called saturation, whereas the slope in the PCC and PMC continuously increases along the intensity level (Fig. 3). Saturation is particularly susceptible to varying methodological conditions and has been documented when stimuli were presented at shorter intervals than 2.5 s or when the intensity was held constant within blocks (Näätänen and Picton, 1987). However, this effect is discussed controversially to occur in the auditory cortex. While some studies reported saturation effects (Bruneau et al., 1985; Lockwood et al., 1999; Neukirch et al., 2002; Reite et al., 1982) others did not (Brechmann et al., 2002; Hall et al., 2001; Hart et al., 2002; Jäncke et al., 1998; Langers et al., 2007; Soeta and Nakagawa, 2009). Thus it appears that the mechanism leading to saturation is not well understood. The hypothesis of intensity selectivity of neurons contribute to sorting out this issue: first, the observation of spatial extend of activated voxels with increasing intensities in fMRI leads to the hypothesis of an increase in the number of responding neurons. As a consequence, involved neurons spread to auditory association areas when the monotonic neurons in PAC are saturated (Jäncke et al., 1998; Uppenkamp and Roehl, 2013). The observed response saturation in PAC in our data might be a consequence of this restricted response. Second, it is supposed that neurons in the auditory cortex have specific functions related to the decomposition of acoustic information (Seifritz et al., 2002). The so called monotonic and non-monotonic intensity tuned neurons differ in their response to intensity level to protect the sensory system from overstimulation and are thought to be topographically organized without forming a clear intensity map in PAC (Ojima, 2011). An incoming sensory stimulus gets processed in these neurons by a cortical intensity tuning mechanism that is based on the basic principle of the canonical microcircuit. This process emphasizes that temporal interaction between excitatory thalamic and inhibitory input via interneurons is pivotal for intensity tuning (Ojima, 2011; Wu et al., 2011). The fact that inhibition is less represented than excitation by the BOLD activation in functional imaging (Waldvogel et al., 2000), having in mind this interactional process, this could explain why most fMRI studies investigating response saturation in PAC did not find a saturation effect.

Interestingly, the characteristics of the activation found in the PMC in our data is in line with earlier observations from our working group: Hagenmuller et al. (2011) revealed that the LDAEP slopes (amplitudes plotted against intensity) differentiate between DSA and single-electrode estimation at Cz. While the slope induced at the scalp showed a steady rise to increasing intensity levels, the potentials within PAC saturated with the highest intensity. This effect is also shown in the present data, when activations over intensities in PAC and PMC are compared. Considering the similar LDAEP slopes at Cz and within the PMC, we can suppose that the single-electrode method's sensitivity to potential changes outside the temporal cortex is affected by this frontal source.

Furthermore, the nature of synchronicity of the activated brain regions plays an important role. Huang et al. (2003) reported a varying percentage of explained variance at the Cz electrode from bilateral superior temporal gyrus (STG) sources between healthy controls and patients with schizophrenia. The authors attributed this group differences to an additional generator outside the STG that is supposed to fire synchronously or asynchronously with the sources in auditory cortex. In the case of synchronously firing – as showed in healthy subjects – it is possible that the variances of both sources were correlated and therefore not detectable at Cz. Interfering contributions from extra-auditory areas, for instance from the PCC, could lead to additional variances of the results across psychiatric disorders complicating the use of different analysis approaches (Jaworska et al., 2013; Park et al., 2011).

Substantive procedural differences make direct comparisons between studies on LDAEP difficult. As discussed by many authors, the stimuli presented to the subject have a crucial impact on the resulting signal and its sources. For example there is a big range of intensity levels presented in LDAEP studies – varying from two to six sound levels – what implicates differences in initial levels that in turn have an impact on the N1m amplitude (Park et al., 2011; Soeta and Nakagawa, 2012). Moreover, as already discussed above the ISI is supposed to have an effect on the appearance of the sources because recovery cycles differ between populations of neurons (Coch et al., 2005). It has even been demonstrated that the way the intervals are presented (randomized or in a block) influences the signal (Zacharias et al., 2012). In our study we did not focus on variation in ISI and its specific effects on source localisation remain open. Furthermore, an effect of frequency on the loudness dependence was reported (Soeta and Nakagawa, 2009).

Further research using dipole source analysis that takes this prior knowledge about the generating sources into account, will need to be undertaken. Sophisticated Bayesian inversion schemes (Kiebel et al., 2008) are useful to objectively compare competing dipole models that vary in the numbers of dipoles or other informative priors and decide which theory explains the observed data best.

Conclusions

This study concentrates on the underlying mechanism of activation during the processing of auditory evoked fields related to the variation of tone intensities. Our results indicate that apart from the auditory cortex and its association areas other regions are activated post stimulus in the time window of N1m and P2m. The most striking result to emerge from the data is additional activation in the premotor (PMC) and primary somatosensory areas with the highest intensity levels. Moreover, we found loudness dependent activation in the posterior cingulate cortex (PCC). For further investigation we analyzed time courses of the activity and receptiveness to rising intensity levels in these areas. The motor response might originate from a reaction (e.g. attentional, orienting or protective) of the organism to exceptional stimuli and is most likely indicated at the scalp level near vertex. As a result, source localization and single-electrode estimation do not cover the same sources and we suggest that these methods are not directly comparable in the analysis of LDAEP.

Acknowledgments

This research was partially funded by EMDO foundation (EMDO Stiftung Zurich, grant number 784), grant coordinated by WK. CW is supported by the Swiss National Science Foundation (SNSF grant P1ZHP3_148704 and PBZHP3_143640). NJS is funded in part by the Helmholtz Alliance ICEMED — Imaging and Curing Environmental Metabolic Diseases, through the Initiative and Network Fund of the Helmholtz Association.

No funding body was involved in the design of experiment, data collection and analysis, interpretation of the results or preparation and submission of the manuscript. The authors declare that they have no conflict of interest.

References

Alcaini, M., Giard, M., Thevenet, M., Pernier, J., 1994. Two separate frontal components in the N1 wave of the human auditory evoked response. Psychophysiology 31, 611–615.

Arezzo, J., Pickoff, A., Vaughan, H.G., 1975. The sources and intracerebral distribution of auditory evoked potentials in the alert rhesus monkey. Brain Res. 90, 57–73.

Attal, Y., Maess, B., Friederici, A., David, O., 2012. Head models and dynamic causal modeling of subcortical activity using magnetoencephalographic/electroencephalographic data. Rev. Neurosci. 23, 85–95.

Azmitia, E.C., Gannon, P.J., 1986. The primate serotonergic system: a review of human and animal studies and a report on *Macaca fascicularis*. Adv. Neurol. 43, 407–468.

Baribeau, J.C., Laurent, J.P., 1987. The effect of selective attention on augmenting/intensity function of the early negative waves of AEPs. Electroencephalogr. Clin. Neurophysiol. Suppl. 40, 68–75.

Brechmann, A., Baumgart, F., Scheich, H., 2002. Sound-level-dependent representation of frequency modulations in human auditory cortex: a low-noise fMRI study. J. Neurophysiol. 87, 423–433.

Bruneau, N., Roux, S., Garreau, B., Lelord, G., 1985. Frontal auditory evoked potentials and augmenting-reducing. Electroencephalogr. Clin. Neurophysiol. 62, 364–371.

Buchsbaum, M., 1971. Individual differences in stimulus intensity response. Psychophysiology 8, 600–611.

Chen, Y.-H., Dammers, J., Boers, F., Leiberg, S., Edgar, J.C., Roberts, T., Mathiak, K., 2009. The temporal dynamics of insula activity to disgust and happy facial expressions: a magnetoencephalography study. Neuroimage 47, 1921.

Coch, D., Skendzel, W., Neville, H.J., 2005. Auditory and visual refractory period effects in children and adults: an ERP study. Clin. Neurophysiol. 116, 2184–2203.

Dammers, J., Ioannides, A.A., 2000. Neuromagnetic localization of CMV generators using incomplete and full-head biomagnetometer. Neuroimage 11, 167–178.

Dammers, J., Mohlberg, H., Boers, F., Tass, P., Amunts, K., Mathiak, K., 2007. A new toolbox for combining magnetoencephalographic source analysis and cytoarchitectonic probabilistic data for anatomical classification of dynamic brain activity. Neuroimage 34, 1577–1587.

Dammers, J., Schiek, M., Boers, F., Silex, C., Zvyagintsev, M., Pietrzyk, U., Mathiak, K., 2008. Integration of amplitude and phase statistics for complete artifact removal in independent components of neuromagnetic recordings. IEEE Trans. Biomed. Eng. 55, 2353–2362.

De Pascalis, V., Cozzuto, G., Russo, E., 2012. Effects of personality trait emotionality on acoustic startle response and prepulse inhibition including N100 and P200 event-related potential. Clin. Neurophysiol. 124, 292–305.

Debener, S., Strobel, A., Kurschner, K., Kranczioch, C., Hebenstreit, J., Maercker, A., Beauducel, A., Brocke, B., 2002. Is auditory evoked potential augmenting/reducing affected by acute tryptophan depletion? Biol. Psychiatry 59, 121–133.

Eickhoff, S.B., Heim, S., Zilles, K., Amunts, K., 2006. Testing anatomically specified hypotheses in functional imaging using cytoarchitectonic maps. Neuroimage 32, 570–582.

Elberling, C., Bak, C., Kofoed, B., Lebech, J., Saermark, K., 1982. Auditory magnetic fields from the human cerebral cortex: location and strength of an equivalent current dipole. Acta Neurol. Scand. 65, 553–569.

Fink, M., Wadsak, W., Savli, M., Stein, P., Moser, U., Hahn, A., Mien, L.-K., Kletter, K., Mitterhauser, M., Kasper, S., Lanzenberger, R., 2009. Lateralization of the serotonin-1A receptor distribution in language areas revealed by PET. Neuroimage 45, 598–605.

Gallinat, J., Senkowski, D., Wernicke, C., Juckel, G., Becker, I., Sander, T., Smolka, M., Hegerl, U., Rommelspacher, H., Winterer, G., 2003. Allelic variants of the functional promoter polymorphism of the human serotonin transporter gene is associated with auditory cortical stimulus processing. Neuropsychopharmacology 28, 530–532.

Giard, M.H., Perrin, F., Echallier, J.F., Thevenet, M., Froment, J.C., Pernier, J., 1994. Dissociation of temporal and frontal components in the human auditory N1 wave: a scalp current density and dipole model analysis. Electroencephalogr. Clin. Neurophysiol. 92, 238–252.

Godey, B., Schwartz, D., De Graaf, J., Chauvel, P., Liegeois-Chauvel, C., 2001. Neuromagnetic source localization of auditory evoked fields and intracerebral evoked potentials: a comparison of data in the same patients. Clin. Neurophysiol. 112, 1850–1859.

Hagenmuller, F., Hitz, K., Darvas, F., Kawohl, W., 2011. Determination of the loudness dependence of auditory evoked potentials: single-electrode estimation versus dipole source analysis. Hum. Psychopharmacol. Clin. 26, 147–154.

Hahn, A., Wadsak, W., Windischberger, C., Baldinger, P., Höflich, A.S., Losak, J., Nics, L., Philippe, C., Kranz, G.S., Kraus, C., 2012. Differential modulation of the default mode network via serotonin-1A receptors. Proc. Natl. Acad. Sci. U. S. A. 109, 2619–2624.

Hall, D.A., Haggard, M.P., Summerfield, A.Q., Akeroyd, M.A., Palmer, A.R., Bowtell, R.W., 2001. Functional magnetic resonance imaging measurements of sound-level encoding in the absence of background scanner noise. J. Acoust. Soc. Am. 109, 1559–1570.

Hari, R., Kaila, K., Katila, T., Tuomisto, T., Varpula, T., 1982. Interstimulus interval dependence of the auditory vertex response and its magnetic counterpart: implications for their neural generation. Electroencephalogr. Clin. Neurophysiol. 54, 561–569.

Hart, H.C., Palmer, A.R., Hall, D.A., 2002. Heschl's gyrus is more sensitive to tone level than non-primary auditory cortex. Hear. Res. 171, 177–190.

Hegerl, U., Juckel, G., 1993. Intensity dependence of auditory evoked potentials as an indicator of central serotonergic neurotransmission: a new hypothesis. Biol. Psychiatry 33, 173–187.

Hegerl, U., Gallinat, J., Mrowinski, D., 1994. Intensity dependence of auditory evoked dipole source activity. Int. J. Psychophysiol. 17, 1–13.

Hitz, K., Heekeren, K., Obermann, C., Huber, T., Juckel, G., Kawohl, W., 2011. Examination of the effect of acute levodopa administration on the loudness dependence of auditory evoked potentials (LDAEP) in humans. Psychopharmacology (Berlin) 1–8.

Huang, M., Edgar, J., Thoma, R., Hanlon, F., Moses, S., Lee, R., Paulson, K., Weisend, M., Irwin, J., Bustillo, J., 2003. Predicting EEG responses using MEG sources in superior temporal gyrus reveals source asynchrony in patients with schizophrenia. Clin. Neurophysiol. 114, 835–850.

Ioannides, A.A., 1995. Estimates of 3D Brain Activity ms by ms From Biomagnetic Signals: Method (MFT), Results and Their Significance. In: Eiselt, E., Zwiener, U., Witte, H. (Eds.), Quantitative and topological EEG and MEG analysis. Universitaetsverlag Druchhaus-Maayer GmbH, Jena, Germany, pp. 59–68.

Ioannides, A.A., 2006. Magnetoencephalography as a research tool in neuroscience: state of the art. Neuroscientist 12, 524–544.

Ioannides, A.A., Bolton, J., Clarke, C., 1990. Continuous probabilistic solutions to the biomagnetic inverse problem. Inverse Prob. 6, 523.

Ioannides, A.A., Liu, M., Liu, L., Bamidis, P., Hellstrand, E., Stephan, K., 1995. Magnetic field tomography of cortical and deep processes: examples of "real-time mapping" of averaged and single trial MEG signals. Int. J. Psychophysiol. 161–175.

Ioannides, A.A., Poghosyan, V., Dammers, J., Streit, M., 2004. Real-time neural activity and connectivity in healthy individuals and schizophrenia patients. Neuroimage 23, 473–482.

Jacobs, B.L., Azmitia, E.C., 1992. Structure and function of the brain-serotonin system. Physiol. Rev. 72, 165–229.

Jäncke, L., Shah, N.J., Posse, S., Grosse-Ryuken, M., Müller-Gärtner, H.W., 1998. Intensity coding of auditory stimuli: an fMRI study. Neuropsychologia 36, 875–883.

Jaworska, N., Blondeau, C., Tessier, P., Norris, S., Fusee, W., Blier, P., Knott, V., 2013. Response prediction to antidepressants using scalp and source-localized loudness dependence of auditory evoked potential (LDAEP) slopes. Prog. Neuropsychopharmacol. Biol. Psychiatry 44, 100–107.

Juckel, G., Molnar, M., Hegerl, U., Csepe, V., Karmos, G., 1997. Auditory-evoked potentials as indicator of brain serotonergic activity — first evidence in behaving cats. Biol. Psychiatry 41, 1181–1195.

Juckel, G., Pogarell, O., Augustin, H., Mulert, C., Müller-Siecheneder, F., Frodl, T., Mavrogiorgou, P., Hegerl, U., 2007. Differential prediction of first clinical response to serotonergic and noradrenergic antidepressants using the loudness dependence of auditory evoked potentials in patients with major depressive disorder. J. Clin. Psychiatry 68, 1206–1212.

Juckel, G., Kawohl, W., Giegling, I., Mavrogiorgou, P., Winter, C., Pogarell, O., Mulert, C., Hegerl, U., Rujescu, D., 2008. Association of catechol-O-methyltransferase variants with loudness dependence of auditory evoked potentials. Hum. Psychopharmacol. 23, 115–120.

Kähkönen, S., Jääskeläinen, I.P., Pennanen, S., Liesivuori, J., Ahveninen, J., 2002. Acute trytophan depletion decreases intensity dependence of auditory evoked magnetic N1/P2 dipole source activity. Psychopharmacology (Berlin) 164, 221–227.
Kawohl, W., Hegerl, U., Müller-Oerlinghausen, B., Juckel, G., 2008. Insights in the central serotonergic function in patients with affective disorders. Neuropsychiatry 22, 23.
Kenemans, J.L., Kähkönen, S., 2011. How human electrophysiology informs psychopharmacology: from bottom-up driven processing to top-down control. Neuropsychopharmacology 36, 26–51.
Kiebel, S.J., Daunizeau, J., Phillips, C., Friston, K.J., 2008. Variational Bayesian inversion of the equivalent current dipole model in EEG/MEG. Neuroimage 39, 728–741.
Kim, Y.H., Gitelman, D.R., Nobre, A.C., Parrish, T.B., LaBar, K.S., Mesulam, M.M., 1999. The large-scale neural network for spatial attention displays multifunctional overlap but differential asymmetry. Neuroimage 9, 269–277.
Knight, R.T., Hillyard, S.A., Woods, D.L., Neville, H.J., 1980. The effects of frontal and temporal-parietal lesions on the auditory evoked potential in man. Electroencephalogr. Clin. Neurophysiol. 50, 112–124.
Kraus, C., Ganger, S., Losak, J., Hahn, A., Savli, M., Kranz, G.S., Baldinger, P., Windischberger, C., Kasper, S., Lanzenberger, R., 2014. Gray matter and intrinsic network changes in the posterior cingulate cortex after selective serotonin reuptake inhibitor intake. Neuroimage 84, 236–244.
Lang, P.J., Bradley, M.M., Cuthbert, B.N., 1990. Emotion, attention, and the startle reflex. Psychol. Rev. 97, 377.
Langers, D.R., van Dijk, P., Schoenmaker, E.S., Backes, W.H., 2007. fMRI activation in relation to sound intensity and loudness. Neuroimage 35, 709–718.
Leech, R., Sharp, D.J., 2014. The role of the posterior cingulate cortex in cognition and disease. Brain 137, 12–32.
Lehmann, D., Skrandies, W., 1980. Reference-free identification of components of checkerboard-evoked multichannel potential fields. Electroencephalogr. Clin. Neurophysiol. 48, 609–621.
Lewis, D.A., Campbell, M.J., Foote, S.L., Morrison, J.H., 1986. The monoaminergic innervation of primate neocortex. Hum. Neurobiol. 5, 181–188.
Linka, T., Müller, B.W., Bender, S., Sartory, G., 2004. The intensity dependence of the auditory evoked N1 component as a predictor of response to Citalopram treatment in patients with major depression. Neurosci. Lett. 367, 375–378.
Lockwood, A.H., Salvi, R.J., Coad, M.L., Arnold, S.A., Wack, D.S., Murphy, B., Burkard, R.F., 1999. The functional anatomy of the normal human auditory system: responses to 0.5 and 4.0 kHz tones at varied intensities. Cereb. Cortex 9, 65–76.
Matthews, S.C., Simmons, A.N., Strigo, I.A., Arce, E., Stein, M.B., Paulus, M.P., 2010. Escitalopram attenuates posterior cingulate activity during self-evaluation in healthy volunteers. Psychiatry Res. 182, 81–87.
Michel, C.M., Murray, M.M., Lantz, G., Gonzalez, S., Spinelli, L., Grave de Peralta, R., 2004. EEG source imaging. Clin. Neurophysiol. 115, 2195–2222.
Mulert, C., Juckel, G., Augustin, H., Hegerl, U., 2002. Comparison between the analysis of the loudness dependency of the auditory N1/P2 component with LORETA and dipole source analysis in the prediction of treatment response to the selective serotonin reuptake inhibitor citalopram in major depression. Clin. Neurophysiol. 113, 1566–1572.
Mulert, C., Jäger, L., Propp, S., Karch, S., Störmann, S., Pogarell, O., Möller, H.J., Juckel, G., Hegerl, U., 2005. Sound level dependence of the primary auditory cortex: simultaneous measurement with 61-channel EEG and fMRI. Neuroimage 28, 49–58.
Näätänen, R., Picton, T., 1987. The N1 wave of the human electric and magnetic response to sound: a review and an analysis of the component structure. Psychophysiology 24, 375–425.
Neukirch, M., Hegerl, U., Kötitz, R., Dorn, H., Gallinat, U., Herrmann, W.M., 2002. Comparison of the amplitude/intensity function of the auditory evoked N1m and N1 components. Neuropsychobiology 45, 41–48.
Neuner, I., Stoecker, T., Kellermann, T., Ermer, V., Wegener, H.P., Eickhoff, S.B., Schneider, F., Shah, N.J., 2010. Electrophysiology meets fMRI: neural correlates of the startle reflex assessed by simultaneous EMG-fMRI data acquisition. Hum. Brain Mapp. 31, 1675–1685.
Neuner, I., Kawohl, W., Arrubla, J., Warbrick, T., Wyss, C., Hitz, K., Boers, F., Shah, J.N., 2014. Cortical signal variation in the processing of rising sound pressure levels: a combined event-related potentials and fMRI study. PLoS One (under review).
Nichols, T.E., Holmes, A.P., 2002. Nonparametric permutation tests for functional neuroimaging: a primer with examples. Hum. Brain Mapp. 15, 1–25.
Ojima, H., 2011. Interplay of excitation and inhibition elicited by tonal stimulation in pyramidal neurons of primary auditory cortex. Neurosci. Biobehav. Rev. 35, 2084–2093.
Oldfield, R.C., 1971. The assessment and analysis of handedness: the Edinburgh inventory. Neuropsychologia 9, 97–113.
O'Neill, B.V., Croft, R.J., Nathan, P.J., 2008. The loudness dependence of the auditory evoked potential (LDAEP) as an in vivo biomarker of central serotonergic function in humans: rationale, evaluation and review of findings. Hum. Psychopharmacol. Clin. 23, 355–370.
Ostermann, J., Uhl, I., Köhler, E., Juckel, G., Norra, C., 2012. The loudness dependence of auditory evoked potentials and effects of psychopathology and psychopharmacotherapy in psychiatric inpatients. Hum. Psychopharmacol. Clin. 27, 595–604.
Park, Y.M., Lee, S.H., Kim, S., Bae, S.M., 2010. The loudness dependence of the auditory evoked potential (LDAEP) in schizophrenia, bipolar disorder, major depressive disorder, anxiety disorder, and healthy controls. Prog. Neuropsychopharmacol. Biol. Psychiatry 34, 313–316.
Park, Y.M., Kim, D.W., Kim, S., Im, C.H., Lee, S.H., 2011. The loudness dependence of the auditory evoked potential (LDAEP) as a predictor of the response to escitalopram in patients with generalized anxiety disorder. Psychopharmacology (Berlin) 213, 625–632.
Parvizi, J., Van Hoesen, G.W., Buckwalter, J., Damasio, A., 2006. Neural connections of the posteromedial cortex in the macaque. Proc. Natl. Acad. Sci. U. S. A. 103, 1563–1568.
Picton, T.W., Alain, C., Woods, D.L., John, M.S., Scherg, M., Valdes-Sosa, P., Bosch-Bayard, J., Trujillo, N.J., 1999. Intracerebral sources of human auditory-evoked potentials. Audiol. Neuro Otol. 4, 64–79.
Reite, M., Zimmerman, J.T., Edrich, J., Zimmerman, J.E., 1982. Auditory evoked magnetic fields: response amplitude vs. stimulus intensity. Electroencephalogr. Clin. Neurophysiol. 54, 147–152.
Schechter, G., Buchsbaum, M., 1973. The effects of attention, stimulus intensity, and individual differences on the average evoked response. Psychophysiology 10, 392–400.
Scherg, M., Berg, P., 1991. Use of prior knowledge in brain electromagnetic source analysis. Brain Topogr. 4, 143–150.
Scherg, M., Picton, T.W., 1991. Separation and identification of event-related potential components by brain electric source analysis. Electroencephalogr. Clin. Neurophysiol. Suppl. 42, 24–37.
Scherg, M., Von Cramon, D., 1985. Two bilateral sources of the late AEP as identified by a spatio-temporal dipole model. Electroencephalogr. Clin. Neurophysiol. 62, 32–44.
Schroeder, C.E., Foxe, J., 2005. Multisensory contributions to low-level, 'unisensory' processing. Curr. Opin. Neurobiol. 15, 454–458.
Seifritz, E., Esposito, F., Hennel, F., Mustovic, H., Neuhoff, J.G., Bilecen, D., Tedeschi, G., Scheffler, K., Di Salle, F., 2002. Spatiotemporal pattern of neural processing in the human auditory cortex. Science 297, 1706–1708.
Sheehan, D.V., Lecrubier, Y., Sheehan, K.H., Amorim, P., Janavs, J., Weiller, E., Hergueta, T., Baker, R., Dunbar, G.C., 1998. The Mini-International Neuropsychiatric Interview (MINI): the development and validation of a structured diagnostic psychiatric interview for DSM-IV and ICD-10. J. Clin. Psychiatry 59, 22–33.
Sigalovsky, I.S., Melcher, J.R., 2006. Effects of sound level on fMRI activation in human brainstem, thalamic and cortical centers. Hear. Res. 215, 67–76.
Smith, S.W., 1997. The Scientist and Engineer's Guide to Digital Signal Processing. California Technical Publ., San Diego, California.
Smith, S.M., Nichols, T.E., 2009. Threshold-free cluster enhancement: addressing problems of smoothing, threshold dependence and localisation in cluster inference. Neuroimage 44, 83–98.
Soeta, Y., Nakagawa, S., 2009. Sound level-dependent growth of N1m amplitude with low and high-frequency tones. Neuroreport 20, 548–552.
Soeta, Y., Nakagawa, S., 2012. Auditory evoked responses in human auditory cortex to the variation of sound intensity in an ongoing tone. Hear. Res. 287, 67–75.
Taylor, J.G., Ioannides, A.A., Muller-Gartner, H.W., 1999. Mathematical analysis of lead field expansions. IEEE Trans. Med. Imaging 18, 151–163.
Uppenkamp, S., Roehl, M., 2013. Human auditory neuroimaging of intensity and loudness. Hear. Res. 307, 65–73.
Vasama, J.P., Mäkelä, J.P., Tissari, S.O., Hämäläinen, M.S., 1995. Effects of intensity variation on human auditory evoked magnetic fields. Acta Otolaryngol. (Stockh.) 115, 616–621.
Velasco, M., Velasco, F., 1986. Subcortical correlates of the somatic, auditory and visual vertex activities. II. Referential EEG responses. Electroencephalogr. Clin. Neurophysiol. 63, 62–67.
Vogt, B.A., Finch, D.M., Olson, C.R., 1992. Functional heterogeneity in cingulate cortex: the anterior executive and posterior evaluative regions. Cereb. Cortex 2, 435–443.
Waldvogel, D., van Gelderen, P., Muellbacher, W., Ziemann, U., Immisch, I., Hallett, M., 2000. The relative metabolic demand of inhibition and excitation. Nature 406, 995–998.
Weidner, R., Boers, F., Mathiak, K., Dammers, J., Fink, G.R., 2010. The temporal dynamics of the Muller–Lyer illusion. Cereb. Cortex 20, 1586–1595.
Woods, D.L., 1995. The component structure of the N 1 wave of the human auditory evoked potential. Electroencephalogr. Clin. Neurophysiol. Suppl. 44, 102–109.
Wu, G.K., Tao, H.W., Zhang, L.I., 2011. From elementary synaptic circuits to information processing in primary auditory cortex. Neurosci. Biobehav. Rev. 35, 2094–2104.
Wutzler, A., Winter, C., Kitzrow, W., Uhl, I., Wolf, R.J., Heinz, A., Juckel, G., 2008. Loudness dependence of auditory evoked potentials as indicator of central serotonergic neurotransmission: simultaneous electrophysiological recordings and in vivo microdialysis in the rat primary auditory cortex. Neuropsychopharmacology 33, 3176–3181.
Wyss, C., Hitz, K., Hengartner, M.P., Theodoridou, A., Obermann, C., Uhl, I., Roser, P., Grunblatt, E., Seifritz, E., Juckel, G., Kawohl, W., 2013. The loudness dependence of auditory evoked potentials (LDAEP) as an indicator of serotonergic dysfunction in patients with predominant schizophrenic negative symptoms. PLoS One 8, e68650.
Zacharias, N., Konig, R., Heil, P., 2012. Stimulation-history effects on the M100 revealed by its differential dependence on the stimulus onset interval. Psychophysiology 49, 909–919.
Zilles, K., Palomero-Gallagher, N., Grefkes, C., Scheperjans, F., Boy, C., Amunts, K., Schleicher, A., 2002. Architectonics of the human cerebral cortex and transmitter receptor fingerprints: reconciling functional neuroanatomy and neurochemistry. Eur. Neuropsychopharmacol. 12, 587–599.